Tellus (1995), 47A, 747–758
Printed in Belgium – all rights reserved

Copyright © Munksgaard, 1995
TELLUS
ISSN 0280–6495

An examination of pressure tendency mechanisms in an idealized simulation of extratropical cyclogenesis

By PAUL A. HIRSCHBERG*, *Department of Meteorology, Naval Postgraduate School, Monterey, CA 93943-5144, USA* and JAMES D. DOYLE, *Marine Meteorology Division, Naval Research Laboratory, Monterey, CA 93943-5502, USA*

(Manuscript received 29 August 1994; in final form 5 December 1994)

ABSTRACT

A numerical simulation of idealized Type-A extratropical cyclogenesis is used to examine pressure tendency mechanisms following a surface low center through its evolution. It is found that horizontal density advection, which maximizes near a developing tropopause undulation (potential vorticity anomaly), is the primary mechanism by which the density and hydrostatic pressure is reduced in the column above the developing surface low center. The density and pressure tendencies associated with horizontal velocity divergence and vertical mass divergence are an order of magnitude larger than the horizontal advective tendencies but are of opposite sign and tend to offset each other. The residual tendencies that result from combining the horizontal velocity divergence and vertical mass divergence are associated with positive density and pressure tendencies that generally oppose but do not counteract the negative tendencies produced by upper-level horizontal advection until late in the evolution of the cyclone. However, this residual divergence is the primary mechanism for the generation of the upstream low density warm pool over the low portion of the tropopause undulation that is later advected over the surface low. In general, these results are consistent with historical as well as more recent studies that suggest the importance of tropopause-level temperature advection in the promotion of the observed height tendency patterns accompanying the superposition of tropopause- and ground-based potential vorticity anomalies during Type B cyclogenesis. From a hydrostatic tendency perspective, it is concluded that baroclinic instability is a process whereby low density, warm air especially above the tropopause that has formed owing to divergence and vertical motion effects is advected downstream and over low-level baroclinic zones and nascent cyclones. In this framework, Type B is distinguished from Type A cyclogenesis by the existence of an initial reservoir of low density, warm air above a tropopause undulation prior to surface cyclogenesis.

1. Introduction

Over the last decade, there has been a growing consensus (Hoskins et al., 1985) that dynamics occurring near the tropopause are a significant component of at least "Type B" (Petterssen and Smebye, 1971) or nonmodal (Farrell, 1984) extratropical cyclogenesis. However, this emphasis on the lower stratosphere and upper troposphere in relation to cyclogenesis is not new. Before the advent of baroclinic instability theory in the late 1940s, there were numerous studies (Hess, 1945; Godson, 1948; Fleagle, 1948) based on earlier work by Von Ficker (1920) that attempted to link the tropopause to surface cyclogenesis. These investigations did not utilize the potential vorticity (PV) concepts that were later introduced by Kleinschmidt (1950a, b) and are currently in vogue (Davis and Emanuel, 1991), but rather focused on the analysis of hydrostatic pressure and height tendency equations. Although a general result of these "hydrostatic tendency" studies was that large density change, divergence, and

* Corresponding author address: Dr. Paul A. Hirschberg, Meteorology Department, Code MR/Hs, 589 Dyer Rd, Room 254, Monterey, CA 93943-5114, USA.

temperature advection near the tropopause were associated with sea-level pressure falls, the findings were inconclusive owing to the sparsity of data and lack of computational speed and accuracy. These shortcomings, along with the diversion of effort into the arena of baroclinic instability theory, led to the decline of the tendency studies in the 1950s.

Recently, Hirschberg and Fritsch (1991a, b; 1992; 1993a, b and 1994; hereafter referred to as HF91a, b; HF92; HF93a, b and HF94, respectively) have revisited the historical hydrostatic tendency approach to understanding the influence of the tropopause region on extratropical cyclones with the modern advantages of increased data resolution, dynamical consistency and computational capability. Their results suggest the importance of tropopause-level temperature advection in the promotion of the observed height tendency patterns accompanying the superposition of tropopause- and ground-based PV anomalies during Type B cyclogenesis. In this paper, we pursue this hydrostatic tendency approach further by investigating how upper-level horizontal density advections associated with a developing tropopause undulation (PV anomaly) affected the evolution of an idealized "Type A" (Petterssen and Smebye, 1971) cyclone simulated in a height-coordinate numerical model.

2. Hydrostatic tendency

The dynamics that drive hydrostatic pressure and height tendency are consistent with and implicitly contained within theoretical constructs such as PV thinking. Nevertheless, it still is important to investigate the mechanisms of hydrostatic tendency to glean descriptive and dynamical links between these theoretical formalizations and more classic synoptic development concepts. In particular, it remains desirable to understand how the superposition of PV anomalies reduces atmospheric mass and induces low-level cyclones. Such an undertaking is especially relevant since the physical mechanisms responsible for the necessary mass depletion during cyclogenesis are not completely clear as evidenced by the recent exchange of Steenburgh and Holton (1993) and Hirschberg and Fritsch (1993b), who debate the exact roles of upper-level temperature (density) advection and the secondary circulation.

A hydrostatic explanation for the inducement of Type B cyclones by superposed PV anomalies is constructed by HF91a, b with a top-down integral approach that was introduced in the historical pressure-change studies (Godson, 1948). This approach is contingent on the existence of a stratospheric level of insignificant dynamics (LID) where the height (pressure) tendency may be considered negligible on the space and time scale of cyclones (HF91a, b). Recent evidence for the existence of a LID has been reported by HF92, HF93b, HF94, and Jusem and Atlas (1991), although its presence was first speculated by Raethjen (1939) and Godson (1948). In particular, HF93b find the LID assumption to be valid for hydrostatic quasigeostrophic flow with wavelengths less than approximately 5000 km.

The LID condition simplifies the understanding of hydrostatic tendency. The typical near-zonal height and thermal configuration in the upper atmosphere implies that low centers below the LID must be associated with relatively warm, less dense air between the LID and the low center (Hirschberg and Fritsch, 1993a). Furthermore, consider the following height

$$\frac{\partial z}{\partial t}=\frac{\partial z(P)}{\partial t}=\frac{R}{g}\int_{P}^{P_{\mathrm{L}}}\frac{\partial T}{\partial t}\,\mathrm{d}\ln p, \tag{1}$$

and pressure

$$\frac{\partial p}{\partial t}=\frac{\partial p(Z)}{\partial t}=g\int_{Z}^{Z_{\mathrm{L}}}\frac{\partial \rho}{\partial t}\,\mathrm{d}z, \tag{2}$$

tendency equations, where $T(\rho)$ is virtual temperature (density) and $P(Z)$ is an arbitrary pressure (height) level below the pressure P_{L} (height Z_{L}) level at the LID. These equations show that only local temperature (density) changes above a given isobaric (height) level and below the LID can contribute to local hydrostatic height (pressure) tendency at the isobaric (height) level in question. Therefore, the temperature (density) above low centers must increase (decrease) for intensification occur. The notion that net column warming is important to cyclone development is similar to the paradigm derived from Petterssen development theory (Petterssen, 1956) concerning the effect of net column Laplacian temperature tendency on low-level vorticity tendency.

2.1. Tropopause undulations

Although it is quite apparent that net column warming and density decrease is necessary for hydrostatic low-level height and pressure falls given a LID, it less clear where and how this warming and density decrease takes place. From the isobaric perspective, HF91a, b suggest that the necessary column warming above developing extratropical low centers occurs near the tropopause. In particular, cross sections through developing baroclinic waves (e.g., Fig. 1) often show synoptic-scale tropopause undulations in association with upper-level PV anomalies. Typically, these undulations have vertical amplitudes of over 200 mb and horizontal scales on the order of the baroclinic wave (1000 km). The warm and cold anomalies that lie over the low (positive) and under the high (negative) portions of the undulation (PV anomalies), respectively, are often aligned almost perpendicular to strong upper-level flow such that large horizontal temperature advections are found upstream and over developing cyclones.

HF91a, b conceptualize that the low-level height falls during Type B cyclogenesis events can result from a synergistic interaction that occurs in the presence of a LID as the temperature advection and vertical motion patterns accompanying a tropopause undulation propagate over favorable regions of warm advection and less stable air in the troposphere. According to this model, lower-tropospheric cyclones are hydrostatically induced underneath stratospheric warm pools situated above the low portion of a tropopause PV anomaly (see also Bell and Bosart, 1993) and also under warm anomalies in the troposphere. Subsequent lower-stratospheric warm advection deepens the low-level cyclone, while enhanced high-level divergence and low-level convergence continually fed with moist, less stable air, intensifies the vertical motions. The enhanced vertical circulation, in turn, amplifies the tropopause undulation and rapidly intensifies and deepens the vertical extent of the lower-stratospheric warm advection in association with the amplifying tropopause PV anomaly. Finally, the occlusion process, i.e., the vertical stacking of the surface low with the tropospheric troughs, occurs as the progressive warming of the stratosphere and cooling of the troposphere causes the warmest column of air to be located more directly underneath the stratospheric warm pool.

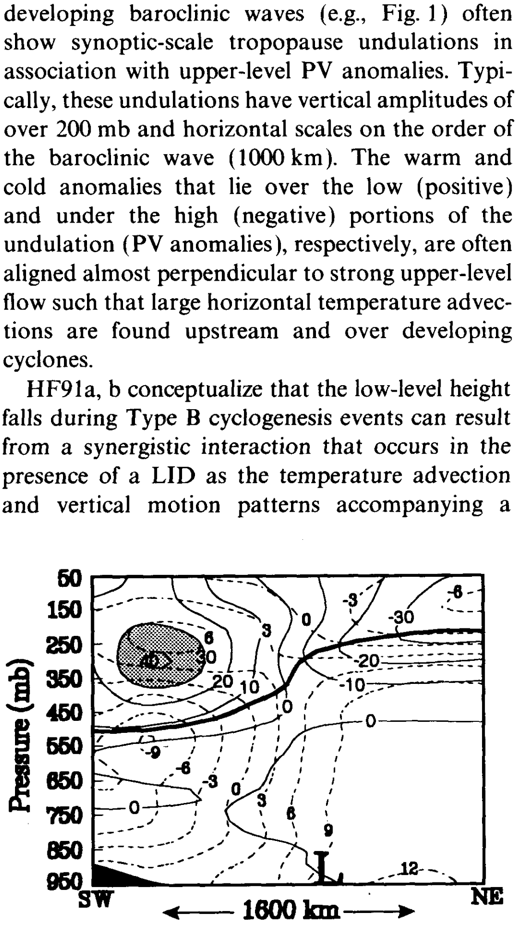

Fig. 1. Cross section southwest (SW) to northeast (NE) of observed deviation (actual minus map-mean) isentropic PV (solid, contour interval 10×10^{-7} m^2 s^{-1} K kg^{-1}) and deviation virtual temperature (dashed, contour interval 3 K). Stippling denotes regions with anomalously high values of PV. The position of the dynamic tropopause (PV value of 10^{-6} m^2 s^{-1} K kg^{-1}) is denoted by a heavy solid line and the position of the surface low by an "L".

2.2. The mechanisms of height tendency

To examine this scenario, HF91a, b studied a rapidly developing Type B continental cyclone with a top-down height tendency equation

$$\frac{\partial z}{\partial t} = \frac{R}{g} \int_{p}^{P_L} (-\boldsymbol{v} \cdot \nabla_p T + \omega s) \, \mathrm{d} \ln p, \tag{3}$$

formed by substituting a form of the thermodynamic equation into (1) and by assuming a LID at $P_L = 50$ mb. They showed that strong upper-level horizontal temperature advection accompanying a tropopause undulation did slightly offset compensating adiabatic cooling by ascent and was responsible for the necessary warming and height falls above the surface low center. The significance of lower-stratospheric temperature advection during Type B cyclogenesis has also been recently reported by Boyle and Bosart (1986), Lupo et al. (1992), Jusem and Atlas (1991), and Martin et al. (1993). In particular, a pressure-time section of local temperature and height tendency (Fig. 2) following the observed cyclone center in HF91a, b indicates the intensification of the lower-stratospheric warming over the low up to the time of maximum sea-level deepening rate (1200 UTC 4

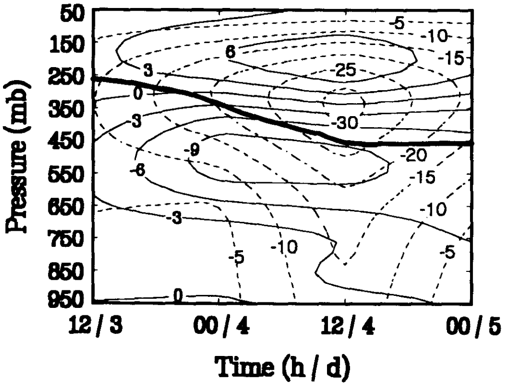

Fig. 2. Pressure-time section of $\partial T/\partial t$ (solid, contour interval 3×10^{-1} K h^{-1}) and $\partial Z/\partial t$ (dashed, contour interval 5 m h^{-1}) following an observed surface low from 1200 UTC 3 January to 0000 UTC 5 January 1982. The position of the dynamic tropopause (PV value of 10^{-6} m^2 s^{-1} K kg^{-1}) is denoted by a heavy solid line.

January 1982) and the associated large height falls directly beneath the warming. Significantly, height falls reach the lower atmosphere despite substantial cooling in the troposphere. Note also that the tropopause descends as the low moves progressively underneath the stratospheric warm pool. Similar relationships between the temperature tendency components and the quasi-geostrophic height tendencies were reported in analytic modeling studies (HF93a and HF94) that furthermore demonstrate the sensitivity of the instantaneous structure and deepening rates of cyclones to the thermal configuration of the tropopause region.

2.3. *The mechanisms of pressure tendency*

The description of cyclogenesis by HF91a, b in terms of isobaric height tendency arises in part from the convenience of evaluating temperature change mechanisms in the thermodynamic equation with the three-dimensional observational and model data operationally available. However, the dynamics that drive hydrostatic tendency should not be coordinate-system dependent. Consequently, the apparent dominance of high-level isobaric temperature advection in driving low-level height tendencies near cyclones should appear in height coordinates as a dominance of high-level density advection in producing low-level pressure tendencies.

Studies (e.g., Bjerknes and Holmboe, 1944; Whitaker et al., 1988) designed to evaluate and understand pressure tendency have focused on the analysis of the so-called tendency equation (Margules, 1904). A version of this equation,

$$\frac{\partial p}{\partial t} = -g \int_{Z}^{Z_L} \nabla \cdot \rho \mathbf{v} \, \mathrm{d}z, \tag{4}$$

can be formed by substituting the continuity equation into (2). While these studies have shown that the necessary mass divergence typically occurs in the upper levels during cyclogenesis, they have not examined which component of the mass divergence dominates, the density advection or the velocity divergence. Recently, Jusem and Atlas (1991) have explored this question by taking advantage of the dynamic consistency of a numerical model to evaluate a numerically-simulated case of rapid Type B cyclogenesis with a Margules-type tendency equation. Consistent with the upper-level isobaric temperature-advection mechanism, they found that the 12-h pressure changes accompanying the cyclogenesis reflected the pattern of vertically-integrated horizontal density advection, which was dominated by the lower tropospheric-lower stratospheric contributions associated with a short-wave trough and tropopause undulation.

To further investigate the upper-level density-advection mechanism, we next examine the instantaneous pressure tendencies in a 240-h numerical simulation of an idealized Type A cyclogenesis with an expanded version of (4). The examination of this Type A cyclogenesis, which may be described as the growth of an unstable normal mode on a baroclinically unstable basic state, represents an extreme test of the upper-level density advection hypothesis since no preexisting tropopause undulation and accompanying low density (warm) pool are present as is the case during the more typical Type B cyclogenesis events.

3. Model

The atmospheric model used is a dry version of the Navy's Coupled Ocean/Atmosphere Mesoscale Prediction System (COAMPS, Hodur, 1993). The three-dimensional model solves the fully compressible, nonhydrostatic equations of motion in a sigma-*z* coordinate system. In this study, the model is used in a channel mode with the f-plane approximation (latitude of 45° N) and no terrain. Surface fluxes of heat and moisture are set to zero. Turbulent mixing is parameterized by a 1.5 order closure method with a predicted turbulent kinetic energy budget. Explicitly predicted variables include perturbation potential temperature, perturbation pressure, and three-dimensional wind components. Here perturbation refers to deviations from the initial mean state that is a function of z only. Forty vertical levels are used with 14 above 18 km (approximately 70 mb) to provide adequate resolution of the lower stratosphere. The horizontal grid dimensions are 4000 km zonally by 6000 km meridionally with a horizontal grid increment of 100 km. The time step is 450 s and the bottom and top boundary conditions are that $w = 0$ at 0 and 45 km, respectively.

The background flow consists of a zonally symmetric jet stream based on winter-mean conditions (Oort, 1983). The maximum wind speed is 40 m s^{-1} near the center of the domain at 11.13 km (approximately 220 mb). The wind is assumed to be near zero at the surface and to decrease to 5 m s^{-1} at 25 km. The temperature distribution is found by applying thermal wind balance to the wind distribution with a temperature profile based on the standard atmospheric lapse rate at the center of the jet. A small meridional wind component below 250 mb, specified as a sinusoidal function with a wavelength of 4000 km that damps near the boundaries, is used to provide the initial perturbation on the baroclinically unstable jet.

4. Results

During the 240-h simulation, a surface low develops, deepens approximately 43 mb and then fills 15 mb (Fig. 3)*. The maximum pressure tendency at the low center approaches 15 mb (24 h)$^{-1}$ between 114 and 138 h. At the time of maximum depth near 174 h, the 970-mb surface cyclone exhibits mature frontal signatures (Fig. 4a). A cross section (Fig. 4b) through the cyclone center at this time shows that the occluded low lies underneath the low portion of a tropopause

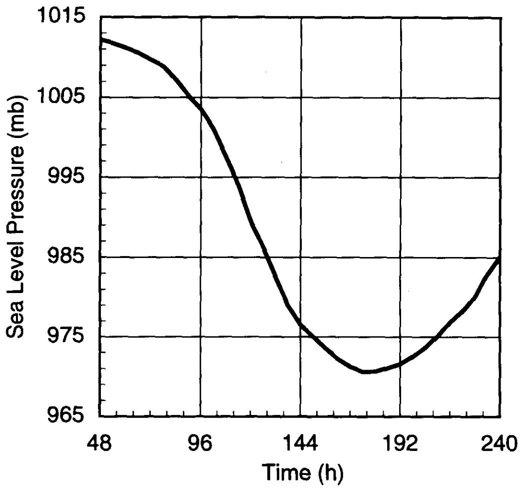

Fig. 3. Pressure trace (mb) at the center of the COAMPS sea-level (surface) cyclone as a function of time (h) from 48 h to 240 h.

undulation (positive PV anomaly) that had formed upstream of the nascent surface cyclone early in the simulation. Characteristically, above the low (high) portion of the undulation, a pool of relatively low (high) density air is present. Near 2 km, a second pool of low density air is centered downstream of the surface low center in association with the strong low-level frontal features that have formed. Height-time sections of the area-average (400 km by 400 km) dynamic tropopause, model-generated* local density (Fig. 5a) and local pressure (Fig. 5b) tendencies following the simulated Type A surface low center displays features that are similar to the analogous pressure-time section (Fig. 3) of the local virtual temperature and local height tendencies following an observed Type B cyclone. The tropopause descends over the low through the deepening portion of the evolution of the storm and ascends as it fills after 174 h. Negative pressure tendencies increase over the low up to 126 h in association with negative density tendencies throughout most of the column. The largest negative pressure tendencies (near

* The first 48 h of simulation are not presented owing to the model spin up during this time interval.

* The model-generated tendencies are obtained every 6 h during the simulation directly from the model by a finite difference of the field in question over two centered time steps.

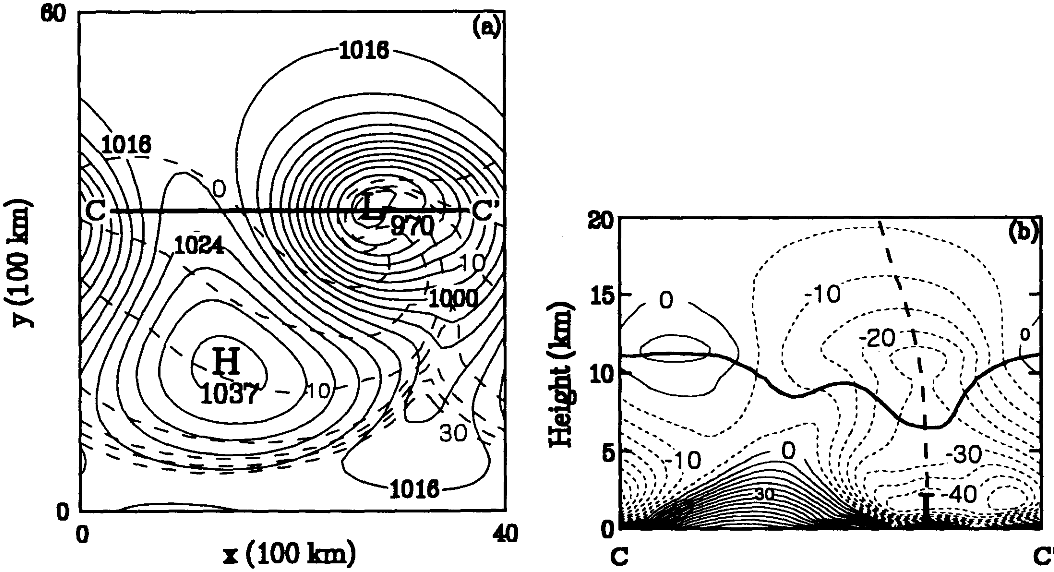

Fig. 4. (a) COAMPS sea-level pressure (solid, contour interval 4 mb) and temperature (dashed, contour interval 5°C) at 174 h; and (b) cross section along C-C′ in (a) of density perturbation (contour interval 10×10^{-3} kg m^{-3}) relative to the background flow. In (a), the central pressures are denoted below the positions of the surface low and high, which are represented by an "L" and "H", respectively. In (b), the surface low position and trough axis is denoted by and an "L" and heavy dashed line, respectively. Solid and dashed contours indicate positive and negative values, respectively. The position of the dynamic tropopause (PV value of 2×10^{-6} m^2 s^{-1} K kg^{-1}) is denoted by a heavy solid line. In this and following figures, perturbation refers to deviations from the initial mean state that is a function of z only.

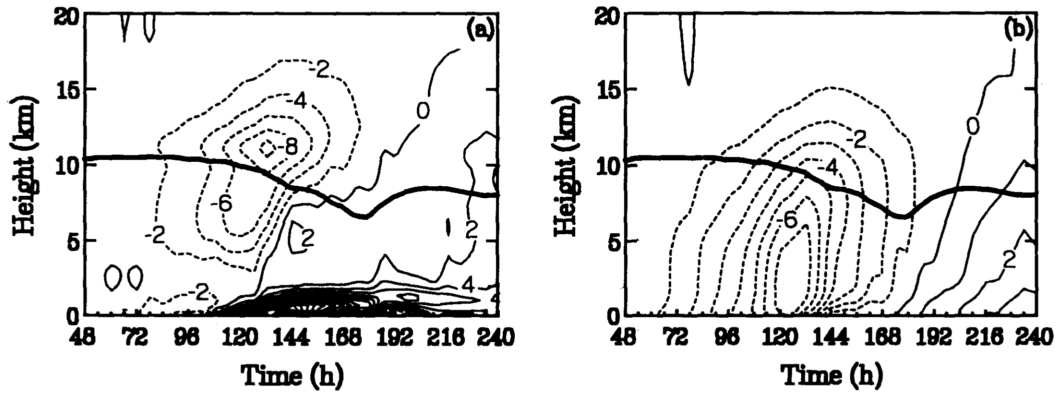

Fig. 5. Height-time section of 400 km by 400 km area average model-generated (a) local density tendency (contour interval 2×10^{-4} kg m^{-3} h^{-1}); and (b) local pressure tendency (contour interval 1×10^{-1} mb h^{-1}) following the COAMPS surface cyclone from 48 h to 240 h. In (a) and (b) solid and dashed contours indicate positive and negative values, respectively. The position of the dynamic tropopause (PV value of 2×10^{-6} m^2 s^{-1} K kg^{-1}) is denoted by a heavy solid line.

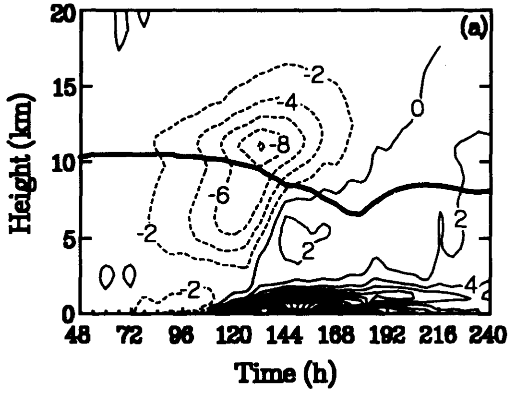

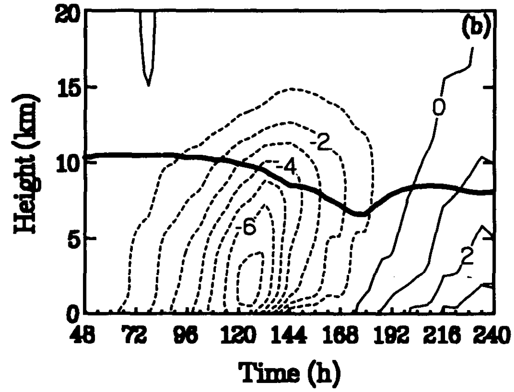

Fig. 6. As in Fig. 5 except for local density and pressure tendencies calculated from (5).

126 h) are generally located in the mid to lower troposphere just below a layer of negative density tendency with maximum negative values located in the lower stratosphere near 11 km and just above the descending tropopause. Below 2 km, the negative pressure tendencies decrease slightly toward the surface in association with a shallow layer of strong positive density tendencies, but remain relatively large and negative. Between 126 h and 174 h, the low continues to lie in an area of negative pressure tendencies and therefore continues to deepen, but at lessening rates as the lower tropospheric layer of positive density tendencies rapidly extends in the vertical and the upper-level negative density tendencies decrease. Thereafter, the layer of positive density tendencies begins to overwhelm the decreasing upper-level negative tendencies as suggested by the positive pressure tendencies appearing near the surface. By 240 h, the whole column above the low experiences density and pressure rises.

To diagnose the mechanisms of hydrostatic pressure tendency that occur over the simulated surface low center, we apply the following pressure tendency equation

$$\frac{\partial p}{\partial t} = g \int_{Z}^{Z_L} \left[-v \cdot \nabla_z \rho - \left(\rho \nabla_z \cdot v + \frac{\partial w \rho}{\partial z} \right) \right] \mathrm{d}z, \quad (5)$$

which is formed by expanding the three-dimensional mass divergence term in (4). The level Z_L is taken to be at the top computation level of the model near 43 km where the model pressure tendencies are found to be exceedingly small. Consistent with the isobaric expression for temperature and height tendency (3) and following the scale analysis of Charney (1947) and Phillips (1990), and the pressure tendency equations of Houghton and Austin (1946) and Jusem and Atlas (1991), the density-tendency components and the corresponding pressure tendencies are partitioned according to those owing to horizontal advection (HA), term 1 on right-hand side of (5), and those due to the combination (DV) of the horizontal velocity divergence (HD), and vertical mass divergence (VD), terms 2 and 3, respectively, on the right-hand side of (5). Comparison of the model-generated local density and pressure tendencies (Fig. 5) with the corresponding tendencies (Fig. 6) computed* with (5) demonstrates the efficacy of the calculation method, the legitimacy of the LID condition, and also the expected hydrostatic nature of the simulation.

In support of the partitioning of (5), the two component terms (HD and VD) that comprise DV are large and opposite following the evolving surface low center (Fig. 7). They combine to produce density (Fig. 8a) and pressure (Fig. 8b) tendencies owing to DV an order of magnitude less than either term individually and consequently on the order of the local tendencies (Fig. 5). Clearly, in agreement with earlier studies (Bjerknes, 1940; Phillips, 1990), the vertical motion term VD can

* The computed tendencies are obtained by applying model-consistent spatial finite difference expressions for (5) with the fields of ρ, v and w output at times consistent with the model-generated tendencies.

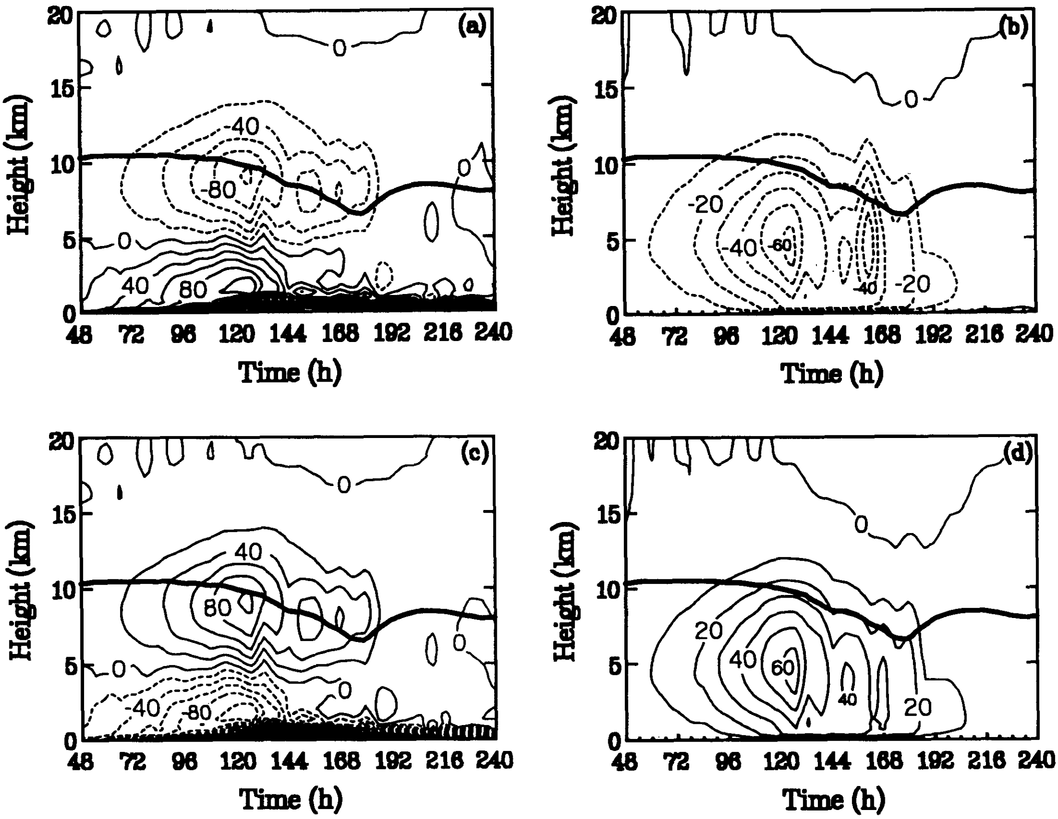

Fig. 7. Height-time section of 400 km by 400 km area-average (a) local density (contour interval 20×10^{-4} kg m^{-3} h^{-1}), and (b) associated local pressure tendencies (contour interval 10×10^{-1} mb h^{-1}) owing to the horizontal velocity divergence HD term in (5); and (c) the local density (contour interval 20×10^{-4} kg m^{-3} h^{-1}), and (d) associated local pressure tendencies (contour interval 10×10^{-1} mb h^{-1}) owing to the vertical mass divergence VD term in (5) following the COAMPS surface cyclone from 48 h to 240 h. In (a)–(d) solid and dashed contours indicate positive and negative values, respectively. The position of the dynamic tropopause (PV value of 2×10^{-6} m^2 s^{-1} K kg^{-1}) is denoted by a heavy solid line.

not be ignored when computing pressure tendency at any level other than at the surface.

Significantly, it is the *upper-level horizontal density advection with maximum negative values near 11 km (approximately 200 mb) and just downstream of the low portion of the developing tropopause undulation (positive PV anomaly) that is primarily responsible for the necessary mass depletion above the low center as it deepens.* In particular, comparison of the patterns of the model-generated local tendencies (Fig. 5) and those owing to HA (Fig. 8c, d) shows that the local tendencies generally reflect but are less intense than the patterns of HA, especially through the deepening stage of the cyclone. Conversely, the height-time section of the tendencies owing to DV (Fig. 8a, b) shows that DV generally contributes to density and pressure rises in the column above the surface cyclone despite a low level shallow layer of negative DV density tendency (Fig. 8a) that migrates upward as time progresses. In particular, pressure rises owing to DV are found at the surface throughout the simulation (Fig. 8b). After the time of maximum deepening near 126 h, the model-generated local tendency patterns (Fig. 5) appear more like the DV patterns as a shallow layer of strong positive density tendency owing to DV (Fig. 8a) expands vertically and combines with a

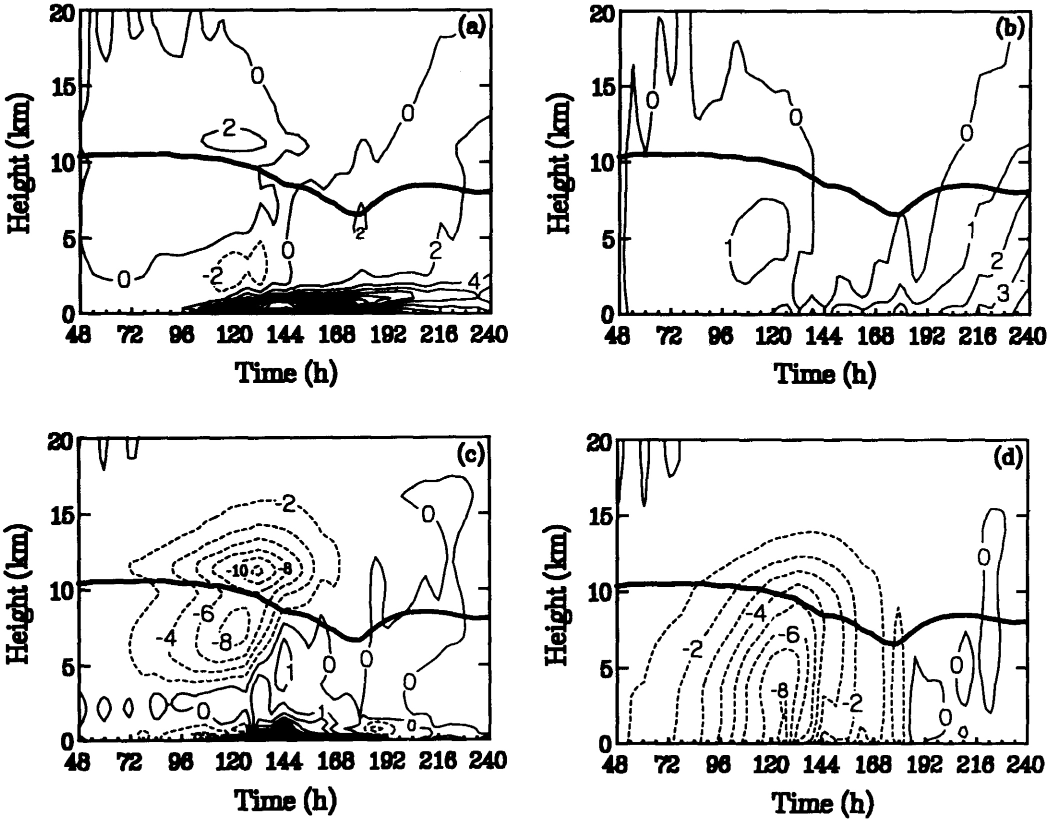

Fig. 8. As in Fig. 7 except for local density and pressure tendencies owing to the combined divergence DV (a) and (b), respectively; and horizontal advection HA (c) and (d), respectively, terms in (5).

less coherent pattern of mid- to lower-tropospheric positive horizontal density advection (Fig. 8c). During this time, the upper-level negative density advection decreases as the low portion of the tropopause undulation becomes superposed over the surface cyclone. Beyond 174 h, the positive tendencies owing to DV and low-level positive HA overwhelm the decreasing upper-level negative HA resulting in positive local pressure tendencies at the surface (Fig. 5b).

In general, these isoheight density and pressure tendency analyses following the COAMPS surface cyclone are similar to isobaric analyses of developing Type B cyclones (e.g., HF91b) that show that the vertical motion-static stability term in (3) and cold tropospheric advection tend to oppose, but not completely offset the warming due to tropopause-level temperature advection in the column above developing surface low centers. Specifically, analogous relationships between HA and DV are found in the present Type A case. Positive density and associated pressure tendency contributions owing to DV (Fig. 8a, b) in conjunction with intensifying positive contributions from HA especially in the lower troposphere (Fig. 8c, d) oppose but do not completely offset the upper-level negative density advections in promoting pressure falls above the surface low until late in the simulation. *Consequently, similar to the isobaric findings, these density tendency results clearly suggest the importance of the prior existence and/or generation of the upper-level low density (warm) pool since it is this air that is later advected over the developing surface low center.* This conclusion is not surprising since the pressure-tendency dynamics must be consistent with the PV explana-

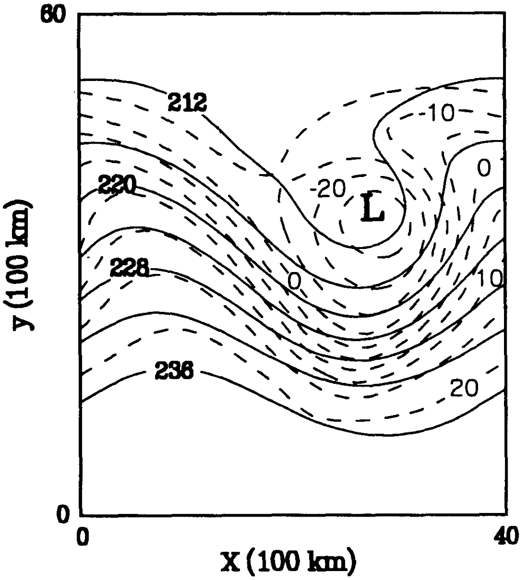

Fig. 9. COAMPS 11.13 km pressure (solid, contour interval 4 mb) and density perturbation (dashed, contour interval 5×10^{-3} kg m^{-3}) analysis at 174 h. The surface low position is denoted by an "L".

tion for extratropical cyclogenesis that highlights the importance of an upper-level PV anomaly typically located along the tropopause (e.g., Hoskins et al., 1985).

Finally, since advection cannot arise until gradients are produced, the effects of divergence and vertical motion must be important to the density and pressure tendency budgets in regions other than in the vicinity of the surface cyclone center. In particular, advection cannot account for the formation and intensification of the closed pool of tropopause-level low density warm air (e.g., Fig. 9) that appears to dominate the density and pressure tendency budget following the surface low. From a thermodynamic perspective, the formation of the warm pool above the low portion of a tropopause undulation occurs in response to the vertical motion-static stability term in (3). Likewise, an analysis of the density tendency components in (5) following the lower-stratospheric density minimum (Fig. 10) during this COAMPS simulation indicates that the mass changes above the low portion of the developing tropopause undulation (positive PV anomaly) is primarily forced by the analogous term DV in (5). Specifically, DV appears to drive the negative local density tendency DT (Fig. 10a) that is responsible for intensifying the negative density perturbation ρ' (Fig. 10b) up to 192 h. This mass depletion above the tropopause occurs as potential vorticity increases. Thereafter, DV becomes positive and the negative density perturbation and potential vorticity decrease.

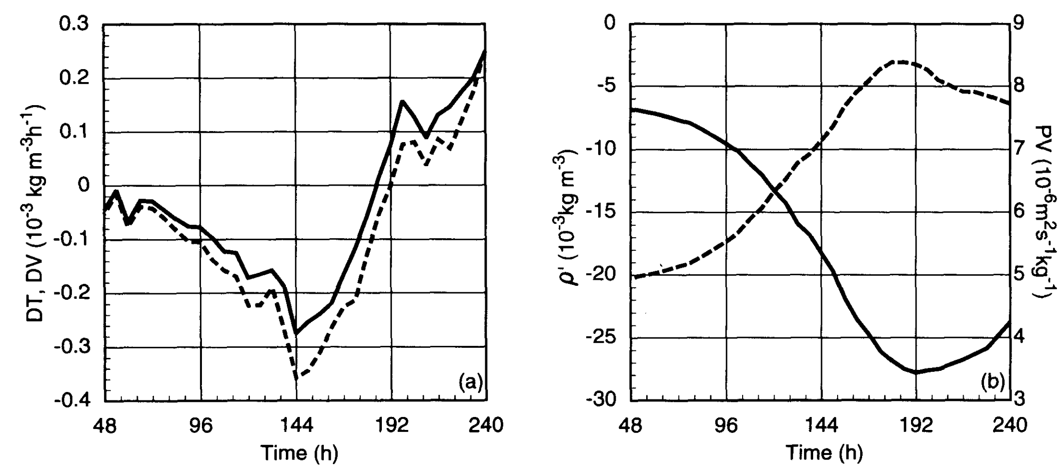

Fig. 10. Volume-average (400 km by 400 km by 1.26 km) of (a) the local density tendency DT (solid, 10^{-3} kg m^{-3} h^{-1}) and the local density tendency owing to DV (dashed, 10^{-3} kg m^{-3} h^{-1}); and (b) the density perturbation ρ' (solid, 10^{-3} kg m^{-3}) and potential vorticity PV (dashed, 10^{-6} m^2 s^{-1} K kg^{-1}) following the density minimum at 11.13 km from 48 h to 240 h.

5. Conclusions

In their overview of refinements in the conceptual models of extratropical cyclones, Shapiro et al. (1991) note that many supposedly new contributions in the field of atmospheric science bear a striking similarity to those of the past, while others often reflect different perspectives of the same physical phenomenon or dynamical process. We have found that is true not only for models of surface cyclones and fronts, but also for dynamics that occur near the tropopause. In particular, some early schools of thought about cyclogenesis (Von Ficker, 1920) focused on lower-stratospheric advection as an important cause of pressure changes at lower levels. Although pressure and height tendency studies in the 1940s showed correlations between this upper-level advection and low-level pressure changes, their results were inconclusive owing to data and computational limitations. In addition, the introduction of baroclinic instability theory shifted the focus to the lower troposphere.

Currently, the relationship between the tropopause region and extratropical cyclogenesis is once again receiving attention, primarily owing to the interpretation of PV dynamics. In this paper, we have revisited the lower-stratospheric/upper-tropospheric advection effects on hydrostatic tendency with the modern advantages of increased data resolution, dynamic consistency, and computational capability by diagnosing pressure tendency mechanisms following the surface low center in an idealized numerical simulation of Type A extratropical cyclogenesis. In agreement with the earlier studies, upper-level horizontal density advection in association with a developing tropopause undulation is the primary mechanism by which the hydrostatic pressure is reduced in the column above the developing surface low center. This result is consistent with more recent studies that have demonstrated the importance of tropopause-level temperature advection in the generation of net-column local warming and isobaric height falls above Type B cyclones, and also compliments PV theory.

Consistent with scale analysis, the density and pressure tendencies associated with horizontal velocity divergence and vertical mass divergence are an order of magnitude larger than the horizontal advective tendencies but are of opposite sign and tend to offset each other. The residual tendencies, owing to the combined horizontal velocity divergence and vertical mass divergence terms, are generally associated with positive tendencies following the surface low that oppose but do not counteract the negative tendencies produced by upper-level advection until late in the evolution of the cyclone. However, the residual divergence is the primary mechanism for the generation of the low density warm pool near the low portion of the tropopause undulation (positive PV anomaly) that is later advected downstream and over the surface low.

Consequently, from a hydrostatic tendency perspective, baroclinic instability is a process whereby low density air especially above the tropopause that has formed owing to divergence and vertical motion effects is advected downstream and over low-level baroclinic zones and nascent cyclones. In this framework, Type B is distinguished from Type A cyclogenesis by the existence of an initial reservoir of low density, warm air above a tropopause undulation prior to surface cyclogenesis.

6. Acknowledgments

This work was supported by the Naval Postgraduate School Direct Research Fund, and by the Naval Research Laboratory Coastal Meteorology ARI program element 0601153N. The authors wish to thank William Blumen, Russell L. Elsberry, Richard M. Hodur, Carlyle H. Wash, and R. T. Williams for their comments and Steven A. Drake, for his technical assistance.

REFERENCES

Bell, G. D. and Bosart, L. F. 1993. A case study diagnosis of the formation of an upper-level cutoff cyclonic circulation over the Eastern United States. *Mon. Wea. Rev.* **121**, 1635–1655.

Bjerknes, J. 1940. The deepening of extra-tropical cyclones. *Quart. J. Roy. Meteor. Soc.* **66**, Supplement, 57–59.

Bjerknes, J. and Holmboe, J. 1944. On the theory of cyclones. *J. Meteor.* **1**, 1–22.

Boyle, J. S. and Bosart, L. F. 1986. Cyclone-anticyclone couplets over North America. Part II: Analysis of a major cyclone event over the eastern United States. *Mon. Wea. Rev.* **114**, 2432–2463.

Charney, J. G. 1947. The dynamics of long waves in a baroclinic westerly current. *J. Meteor.* **4**, 135–163.

Davis, C. A. and Emanuel, K. A. 1991. Potential vorticity diagnostics of cyclogenesis. *Mon. Wea. Rev.* **119**, 1929–1953.

Godson, W. L. 1948. A new tendency equation and its application to the analysis of surface pressure changes. *J. Meteor.* **5**, 227–235.

Farrell, B. F. 1984. Modal and nonmodal baroclinic waves. *J. Atmos. Sci.* **41**, 668–673.

Fleagle, R. G. 1948. Quantitative analysis of factors influencing pressure change. *J. Meteor.* **5**, 281–291.

Hess, S. 1945. A statistical study of the deepening and filling of extratropical cyclones. *J. Meteor.* **2**, 179–184.

Hirschberg, P. A. and Fritsch, J. M. 1991a. Tropopause undulations and the development of extratropical cyclones. Part I: Overview and observations from a cyclone event. *Mon. Wea. Rev.* **119**, 496–517.

Hirschberg, P. A. and Fritsch, J. M. 1991b. Tropopause undulations and the development of extratropical cyclones. Part II: Diagnostic analysis and conceptual model. *Mon. Wea. Rev.* **119**, 518–550.

Hirschberg, P. A. and Fritsch, J. M. 1992. Reply to comments by D. O. Staley. *Mon. Wea. Rev.* **120**, 2402–2404.

Hirschberg, P. A. and Fritsch, J. M. 1993a. A study of the development of extratropical cyclones with an analytic model. Part I: The effects of stratospheric structure. *J. Atmos. Sci.* **50**, 311–327.

Hirschberg, P. A. and Fritsch, J. M. 1993b. On understanding height tendency. *Mon. Wea. Rev.* **121**, 2646–2661.

Hirschberg, P. A. and Fritsch, J. M. 1994. A study of the development of extratropical cyclones with an analytic model. Part II: Sensitivity to tropospheric structure and analysis of height tendency dynamics. *Mon. Wea. Rev.* **122**, 2312–2330.

Hodur, R. M. 1993. *Development and testing of the coupled ocean/atmosphere mesoscale prediction system (COAMPS)*. NRL/MR/7533-93-7213. Naval Research Laboratory, 84 pp.

Houghton, H. G. and Austin, J. M. 1946. A study of non-geostrophic flow with applications to the mechanism of pressure changes. *J. Meteor.* **3**, 57–77.

Hoskins, B. J., McIntyre, M. E. and Robertson, A. W. 1985. On the use and significance of isentropic potential vorticity maps. *Quart. J. Roy. Meteor. Soc.* **111**, 877–946.

Jusem, J. C. and Atlas, R. 1991. Diagnostic evaluation of numerical model simulations using the tendency equation. *Mon. Wea. Rev.* **119**, 2936–2955.

Kleinschmidt, E. 1950a. Uber Aufbau und Entstehung von Zyklonen I. *Meteorol. Rdsch.* **3**, Teil 1, 1–6.

Kleinschmidt, E. 1950b. Uber Aufbau und Entstehung von Zyklonen II. *Meteorol. Rdsch.* **3**, Teil 2, 54–61.

Lupo, A. R., Smith, P. J. and Zwack, P. 1992. A diagnosis of the explosive development of two extratropical cyclones. *Mon. Wea. Rev.* **120**, 1490–1523.

Margules, M. 1904. *Über die Beziehung Zwischen Barometerschwankung un Kontinuitatgleichung*. Boltzman Festschrift, pp. 585–589.

Martin, J. E., Locatelli, J. D. and Hobbs, P. V. 1993. Organization and structure of clouds and precipitation on the mid-Atlantic coast of the United States. Part VI: The synoptic evolution of a deep tropospheric frontal circulation and attendant cyclogenesis. *Mon. Wea. Rev.* **121**, 1299–1316.

Oort, A. H. 1983. *Global atmospheric circulations statistics*, 1958–1973. NOAA Professional Paper 14, 180 pp. [NPIS PB84-129717].

Petterssen, S. 1956. *Weather analysis and forecasting*, 2d edition, Vol. 1. McGraw-Hill, 428 pp.

Petterssen, S. and Smebye, S. J. 1971. On the development of extratropical cyclones. *Quart. J. Roy. Meteor. Soc.* **97**, 457–482.

Phillips, N. A. 1990. The emergence of quasi-geostrophic theory. *The Atmosphere-A challenge. The science of Jule Gregory Charney*, R. S. Lindzen, E. N. Lorenz and G. W. Platzman, (eds.). Amer. Meteor. Soc., pp. 177–206.

Raethjen, P. 1939. Advektive und konvektive, stationare und gegenlaufige Drucanderungen. *Meteor. Z.* **56**, 133–142.

Shapiro, M. A., Donall, E. G., Neiman, P. J., Fedor, L. S. and Gonzalez, N. 1991. Recent refinements in the conceptual models of extratropical cyclones. *First International Symposium on Winter storms.* New Orleans, LA, Amer. Meteor. Soc., pp. 6–14.

Steenburgh, W. J. and Holton, J. R. 1993. The interpretation of geopotential height tendency equations. *Mon. Wea. Rev.* **121**, 2642–2645.

Von Ficker, H. v. 1920. Beziehung zwischen Anderungen des Luftdruckes und der Temperatur in den unteren Schichten der Troposphare (Zusammensetzung der Depressionen). *Sitzber. Akad. Wiss. Wien., Math. Naturn. Kl. Abt. IIa* **129**, 763–810.

Whitaker, J. S., Uccellini, L. W. and Brill, K. F. 1988. A model-based diagnostic study of the rapid development phase of the President's Day cyclone. *Mon. Wea. Rev.* **116**, 2337–2365.